

ELECTRON PARAMAGNETIC RESONANCE STUDIES AND LINEWIDTH ANOMALY OF Cr^{3+} IN SOME FERROELECTRIC ALUMS

RANGNATH NAVALGUND and L. C. GUPTA

Tata Institute of Fundamental Research, Homi Bhabha Road, Bombay 400005, India

(Received 18 August, 1975; in final form 14 January, 1976)

Electron paramagnetic resonance of Cr^{3+} in $\text{CH}_3\text{NH}_3\text{Ga}(\text{SO}_4)_2 \cdot 12\text{H}_2\text{O}$ and $\text{CH}_3\text{NH}_3\text{Al}(\text{SeO}_4)_2 \cdot 12\text{H}_2\text{O}$ (which are known to be ferroelectric) as a function of temperature and orientation has been studied. As one approaches T_c , an anomalous increase of resonance linewidth, which is very pronounced for the satellite transitions has been observed. It is observed experimentally that $\Delta H_c \sim (T - T_c)^{-n}$, where $n \sim 0.4$ for temperatures near to T_c and $n \sim 2.0$ for temperatures further from T_c . The EPR spectrum has also been observed in the ferroelectric phase. It is inferred that the water molecules in the immediate environment of the trivalent metal ion may be playing an important role in the mechanism of ferroelectricity in alums.

I INTRODUCTION

Magnetic resonance and relaxation techniques are important in the investigations of ferroelectric crystals. These studies enable one to gain valuable information about (i) the displacement of atoms and/or the rotation of molecular complexes which occur during the crystallographic phase transition and the resulting change in the symmetry of the crystal and (ii) the dynamical processes that are responsible for the ferroelectric behaviour of the crystal. Rigamonti *et al.*^{1,2} observed a critical increase in the nuclear spin-lattice relaxation rate of Na^{23} in ferroelectric NaNO_2 as one approaches the phase transition temperature. A similar observation was made by Blinc and Zumer in ferroelectric KH_2PO_4 .³ EPR studies have been of particular interest in the case of SrTiO_3 . Oxygen displacements of the order of 4×10^{-3} Å have been detected in this material.⁴ In a series of papers,⁵⁻⁷ Muller *et al.* have described their investigations of EPR linewidth anomalies caused by critical fluctuations near the structural phase transition in this material. They have also obtained the static critical exponents associated with the phase transition. A similar effect was also found in the EPR spectra of Mn^{2+} doped in BaTiO_3 .⁸ Windsch and his coworkers^{9,10} have carried out investigations of the dynamic processes near the ferroelectric phase transition in a number of systems by the electron spin-echo method. EPR linewidth anomaly of V^{2+} near T_c in $\text{K}_4\text{Fe}(\text{CN})_6 \cdot 3\text{H}_2\text{O}$ has also been reported by O'Reilly *et al.*¹¹ Thus, EPR linewidth anomalies of dopant impurity near the ferroelectric

phase transition are of current interest. In this paper, we wish to report the results of our EPR studies of Cr^{3+} in two ferroelectric alums; (i) methyl ammonium gallium sulfate ($\text{CH}_3\text{NH}_3\text{Ga}(\text{SO}_4)_2 \cdot 12\text{H}_2\text{O}$, $T_c = 171$ K, MGSD) and (ii) methyl ammonium aluminium selenate ($\text{CH}_3\text{NH}_3\text{Al}(\text{SeO}_4)_2 \cdot 12\text{H}_2\text{O}$, $T_c = 216$ K, MASED) in which we have observed an anomalous increase of linewidth.

II EXPERIMENTAL

Cr^{3+} doped alums have been grown by the method of slow evaporation of saturated solution containing the constituent sulfates or selenates in stoichiometric ratio. About 0.1% by weight of



was added to the growth solution. Single crystals of the two alums are hexagonal plates with prominent (111) faces. Cr^{3+} doped crystals showed a slight violet colour.

EPR experiments were carried out on a 100 KHz field modulated x-band spectrometer. Crystals of $4 \times 3 \times 2$ mm size were chosen for these experiments. In order to study the rotation pattern of the EPR spectra, the crystals were mounted on a single circle goniometer. The axis of rotation was perpendicular to the direction of the magnetic field. Varian V-4540 variable temperature accessory was used for variable temperature experiments. The temperature could be maintained to $\pm 1^\circ$ and was measured using copper-

constantan thermocouple. A proton probe has been used for magnetic field calibration.

III CRYSTAL STRUCTURE

Alums have the general formula $M^+M_1^{3+}(RO_4)_2 \cdot 12H_2O$ ($M^+ = K, Rb, Cs, NH_4, CH_3NH_3$; $M_1^{3+} = Al, Cr, Fe, Ga, V, In$ and $R = S, Se, Te$). Some of these, in particular those with NH_4^+ or $CH_3NH_3^+$ as monovalent ion M^+ exhibit ferroelectricity.¹² At room temperature the alums possess cubic symmetry and the space group in the paraelectric phase is Pa 3. The unit cell contains four formula units. The immediate environment of the trivalent metal ion M_1 , consists of a trigonally distorted octahedron of water molecules, the trigonal axis being along [111] axis.

IV RESULTS

A. Room Temperature Studies $(3d^3) is^4 F_{3/2}$

The ground state of a free Cr^{3+} ion ~~comprising chromium~~ seven-fold orbital degeneracy and a four-fold spin degeneracy. The cubic crystalline field removes the orbital degeneracy leaving an orbital singlet as the ground state.¹³ The next higher state is approximately $18,000 \text{ cm}^{-1}$ above the ground state. Additional trigonal distortion in the crystal field in conjunction with spin-orbit coupling removes part of the spin degeneracy of the ground state, giving rise to two Kramer's doublets with quantum numbers $M_s = \pm \frac{1}{2}$ and $M_s = \pm \frac{3}{2}$. In the presence of an external magnetic field remaining spin degeneracy is lifted and three allowed ($\Delta M_s = \pm 1$) EPR fine-structure transitions are observed for each Cr^{3+} complex. The transitions ($M_s \rightarrow M_s - 1$), $\pm \frac{3}{2} \rightarrow \pm \frac{1}{2}$ are known as satellite transitions while the transition $\frac{1}{2} \rightarrow -\frac{1}{2}$ is the so called central transition. Naturally occurring chromium comprises mainly of two isotopes ^{52}Cr (isotopic abundance = 84%, nuclear spin $I = 0$) and ^{53}Cr (isotopic abundance = 9.5%, nuclear spin $I = \frac{3}{2}$). The nuclear magnetic moment causes a further splitting of the energy levels of the odd isotope producing three groups of four hyperfine transitions. However, because of the feeble intensity (low abundance) and small splitting (low nuclear magnetic moment) one observes these hyperfine transitions (of ^{53}Cr) only at very low temperatures.¹⁴

From the considerations of ionic radius and valence state, Cr^{3+} is a very suitable paramagnetic ion for EPR studies in alums. (Ionic radii; $Cr^{3+} = 0.64 \text{ \AA}$,

$Al^{3+} = 0.50 \text{ \AA}$, $Ga^{3+} = 0.62 \text{ \AA}$). Cr^{3+} replaces substitutionally the trivalent (M_1^{3+}) in both the alums. Due to the trigonal distortion of the octahedron around Cr^{3+} ion, the four sites become physically non-equivalent. However, all of them are equivalent chemically. As discussed earlier, three allowed EPR fine structure transitions are observed for each of the four magnetically non-equivalent Cr^{3+} ions. Thus along any arbitrary orientation of the crystal with respect to the external magnetic field, twelve lines corresponding to four Cr^{3+} ions have been observed. Figure 1(A) shows the EPR spectrum of Cr^{3+} ion in methyl ammonium gallium sulfate alum for such a direction. The spectrum becomes simple with a magnetic field along [111] axis.

Figure 1(B) shows the spectrum for this orientation. In this orientation, the trigonal axis (principal z axis) of one of the four sites becomes parallel to the direction of the applied magnetic field. The lines a, b and c , shown in Figure 1(B) correspond to the three fine structure transitions of this particular Cr^{3+} complex. The other three sites become magnetically equivalent among themselves and give rise to an identical spectrum marked by d, b and e . EPR of Cr^{3+} in the other alum ($CH_3NH_3Al(SeO_4)_2 \cdot 12H_2O$) shows similar features. Figure 1(C) shows the spectrum of Cr^{3+} in this alum for magnetic field along [111] direction. Figure 2 shows the rotation pattern of Cr^{3+} in $CH_3NH_3Al(SeO_4)_2 \cdot 12H_2O$ in (111) plane. It can be seen from the figure that the entire spectrum repeats after an interval of 60° . It should be noted that the three solid lines do not show any angular dependence in this plane. These lines arise due to Cr^{3+} complex whose principal axis coincides with the rotation axis. Thus it follows that the D tensor is axially symmetric about [111] axis.

The data were analysed using the following spin Hamiltonian.¹⁵

$$H_s = \beta H \cdot g \cdot S + D[S_z^2 - \frac{1}{3}S(S+1)] \quad (1)$$

Expressions evaluated up to second order in D have been used to obtain the spin Hamiltonian parameters and these have been given in Table I.

B. Variable Temperature Studies

In order to study the temperature dependence of the EPR spectrum, the experiments were carried out as a function of temperature. In one of the experiments, the crystal was kept with [111] axis parallel to external magnetic field. The linewidth of both satellite and central transitions (shown in Figures 1(B) and 1(C)) was measured as a function of temperature. The EPR linewidth was observed to exhibit an anomaly as T_c .

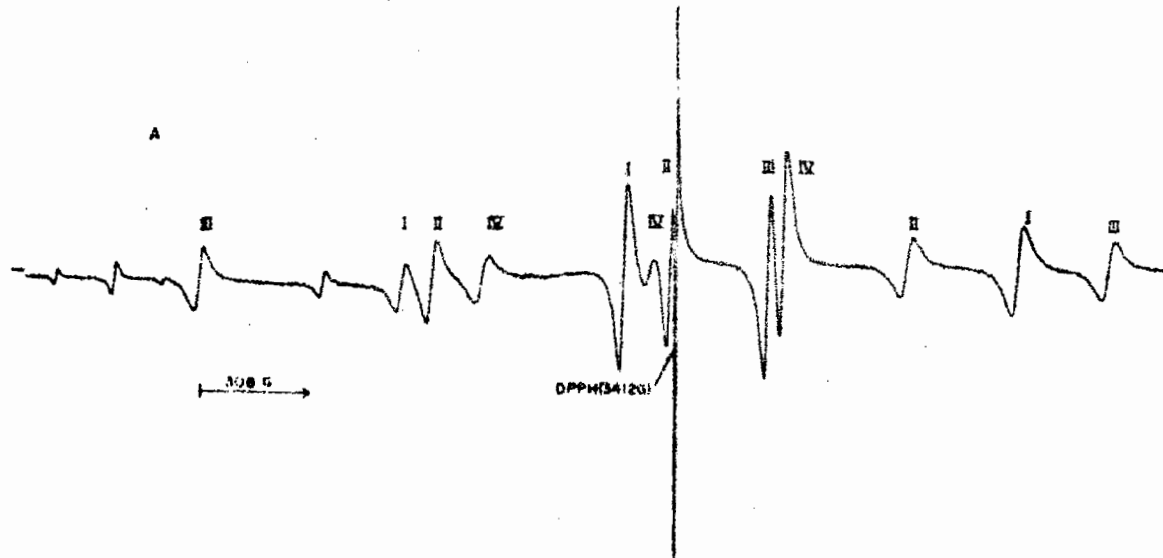


FIGURE 1(A) EPR spectrum of Cr^{3+} in $\text{CH}_3\text{NH}_3\text{Ga}(\text{SO}_4)_2 \cdot 12\text{H}_2\text{O}$ at room temperature with magnetic field direction making an angle of 45° with $[110]$ direction in (111) plane. The transitions marked I, II, III and IV correspond to the four Cr^{3+} complexes.

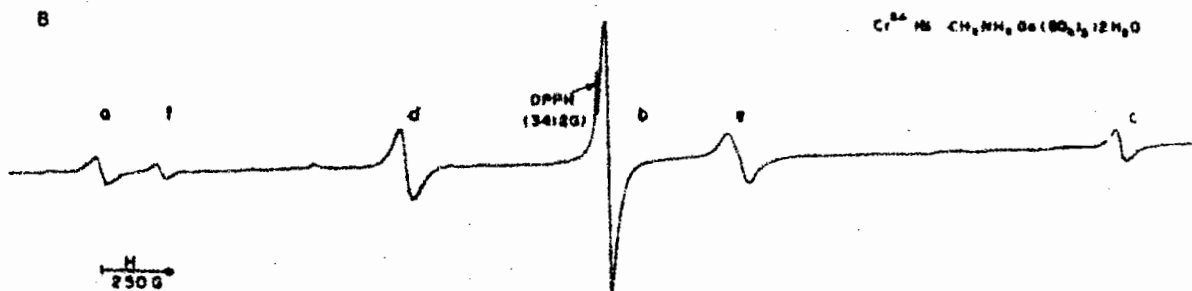


FIGURE 1(B) EPR spectrum of Cr^{3+} in $\text{CH}_3\text{NH}_3\text{Ga}(\text{SO}_4)_2 \cdot 12\text{H}_2\text{O}$ at room temperature with magnetic field along $[111]$ direction, the principal Z axis of complex marked I in Figure 1(A). Lines marked a , b and c belong to this complex. The other three complexes becomes equivalent along this direction and the lines d , b and e correspond to these. d and e contain three lines and b has four lines. The origin of the line marked f is not clear.

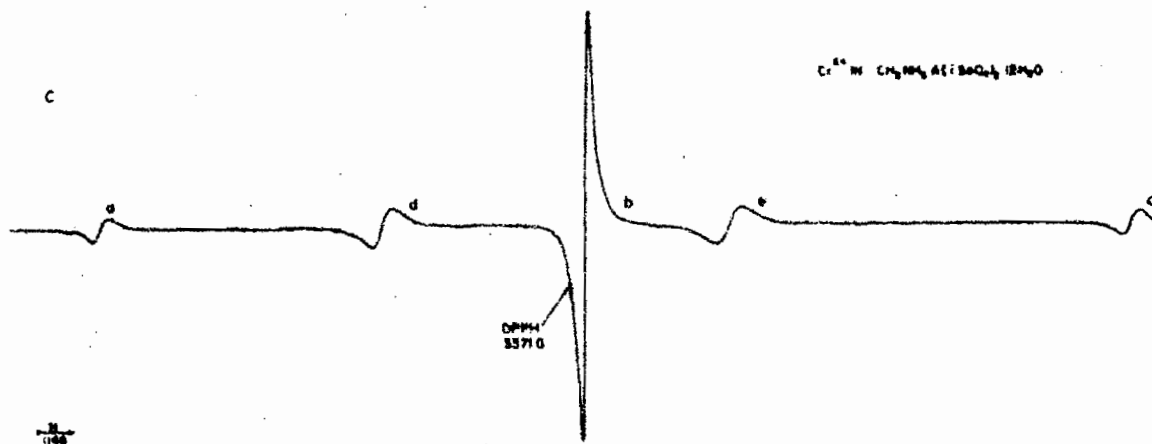


FIGURE 1(C) EPR spectrum of Cr^{3+} in $\text{CH}_3\text{NH}_3\text{Al}(\text{SO}_4)_2 \cdot 12\text{H}_2\text{O}$ for magnetic field along $[111]$ direction.

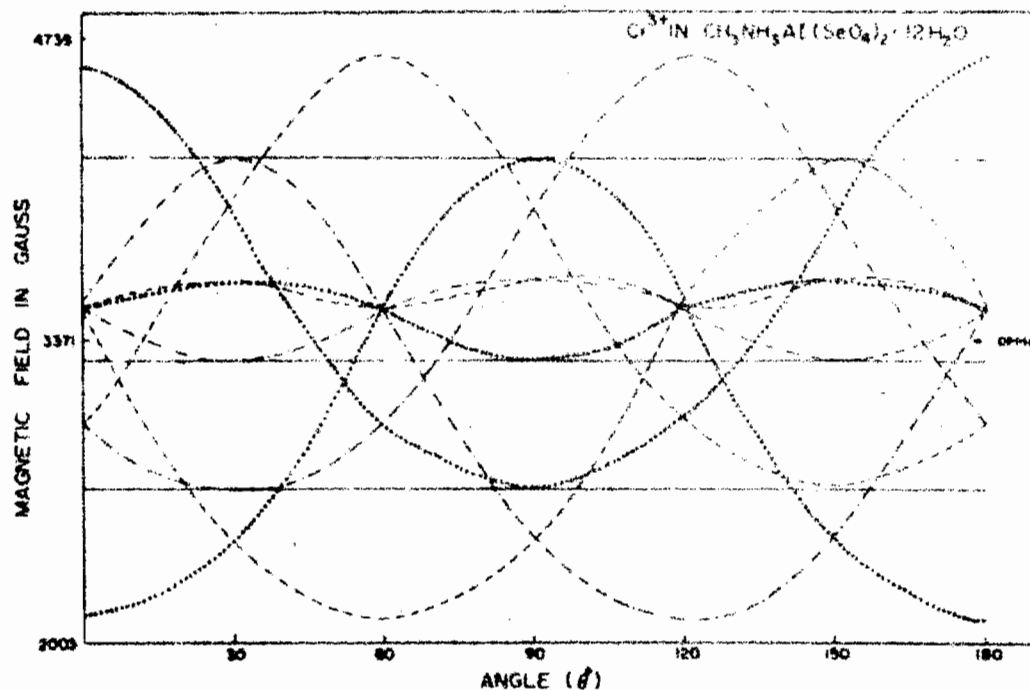


FIGURE 2 Rotation pattern of Cr^{3+} in $\text{CH}_3\text{NH}_3\text{Al}(\text{SeO}_4)_2 \cdot 12\text{H}_2\text{O}$ in (111) plane at room temperature. The horizontal solid lines belong to the complex, whose principal axis coincides with the rotation axis.

TABLE I

Spin Hamiltonian parameters of Cr^{3+} in the two alums at room temperature.

Alum	g_{\parallel}	g_{\perp}	$D(\text{cm}^{-1})$
$\text{CH}_3\text{NH}_3\text{Ga}(\text{SO}_4)_2 \cdot 12\text{H}_2\text{O}$	1.97	1.96	0.082
$\text{CH}_3\text{NH}_3\text{Al}(\text{SeO}_4)_2 \cdot 12\text{H}_2\text{O}$	1.975	1.96	0.072

was approached. Figure 3.1 shows the linewidth behaviour of low field satellite transition and the central transition in MGSD. Similar behaviour is also observed for the high field satellite transition. Figure 3.2 shows the behaviour of the low field satellite transition linewidth in two alums MGSD and MAsE.

EPR experiments have been carried out in the ferroelectric phase also. In this phase, each of the twelve lines shown in Figure 1(A) split into three components. This splitting is consistent with the fact that the spontaneous polarization appears along the cubic axis.¹⁶ The interior of the crystal thus divides into three different regions with the ferroelectric axis parallel to any of the three cube axes of the paraelectric phase. Figure 4 shows, how the four central ($\frac{1}{2} \rightarrow -\frac{1}{2}$) components corresponding to the four Cr^{3+} complexes split into twelve resonance lines as a result of the ferroelectric phase transition. However, the spectrum

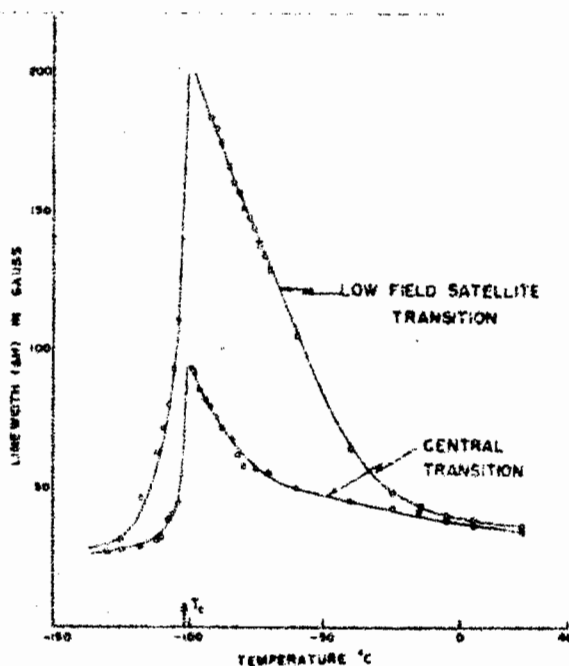


FIGURE 3.1 Linewidth behaviour of both low field satellite transition and central transition in $\text{CH}_3\text{NH}_3\text{Ga}(\text{SO}_4)_2 \cdot 12\text{H}_2\text{O}$.

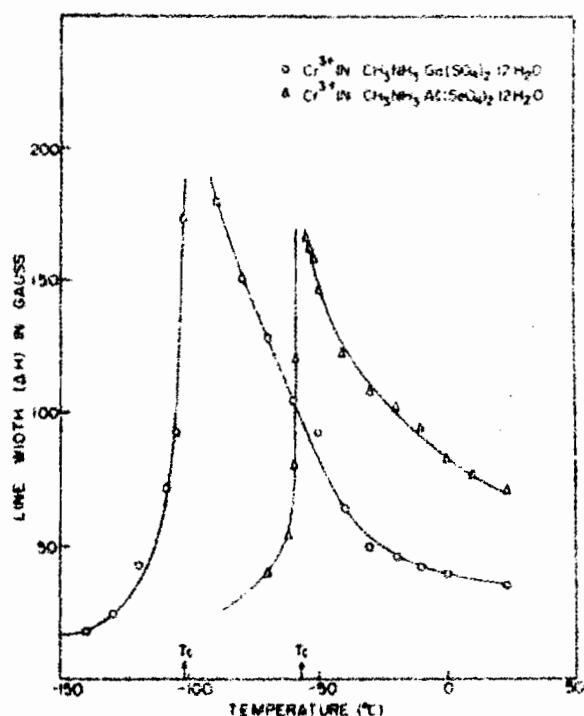


FIGURE 3.2 Linewidth behaviour of low field satellite transition as a function of temperature in the two alums; triangles correspond to MGSD and circles correspond to MASol.

In the ferroelectric phase is quite complex because of three-fold increase in the number of lines. Detailed investigations of the rotation pattern of the entire spectrum therefore in the ferroelectric phase have not been carried out.

V DISCUSSION

The linewidth anomaly in the vicinity of T_c may be explained qualitatively as follows. Well above T_c , the fast fluctuations cause a motional narrowing of the EPR lines. Approaching the phase transition point T_c , the fluctuations are critically slowed down and this leads to the broadening of the EPR lines.⁷ We can estimate the correlation time associated with the fluctuations near T_c in the following way.¹⁷ The Hamiltonian of the system can be written as the sum of two terms.¹⁸

$$\mathcal{H} = g\beta HS_z + \sum_{q=\pm 2, \pm 1, 0} F^{(q)}(\theta, \phi) A^{(q)} \quad (2)$$

where the second term represents the time dependent fluctuating part. The terms $F^{(q)}(\theta, \phi)$ and $A^{(q)}$ are

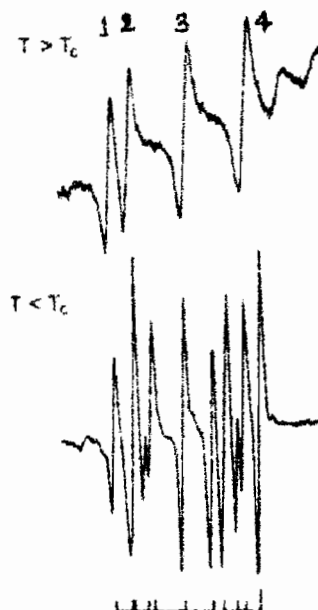


FIGURE 4 EPR spectrum of Cr³⁺ in CH₃NH₃Ga(SO₄)₂·12H₂O above and below the phase transition temperature. The four lines marked 1, 2, 3, 4 in the upper figure correspond to the central transitions of the four complexes in the paraelectric phase. The lower figure shows the splitting of these four into 12 lines in the ferroelectric phase.

defined as in reference (18). The linewidth (ΔH) is inversally proportional to the transverse relaxation time T_2 and is given by the expression.¹⁹

$$-d\langle m+1 | S_x^{-1} | m \rangle / dt = -\frac{1}{T_2} \langle m+1 | S_x | m \rangle \quad (3)$$

$$= -\frac{1}{2} \sum_{q=\pm 2, \pm 1, 0} \langle m+1 | [A^{(-q)}, [A^{(q)}, S_x]] | m \rangle J^{(q)}(i\omega) \quad (4)$$

We obtain,

$$\frac{1}{T_2} = 2J^{(0)} + 12J^{(1)}(\omega); \quad \text{for } (-\frac{1}{2} \rightarrow -\frac{1}{2}) \quad (5)$$

and $(\frac{1}{2} \rightarrow \frac{3}{2})$

and

$$\frac{1}{T_2} = 12J^{(1)}(\omega); \quad \text{for } (-\frac{1}{2} \rightarrow \frac{1}{2}) \quad (6)$$

For a Markovian process with correlation time τ_c

$$J^{(0)} = 2(|F^{(0)}|^2)\tau_c \quad (7)$$

and

$$J^{(1)}(\omega) = 2(|F^{(1)}|^2) \frac{\tau_c}{1 + \omega^2 \tau_c^2} \quad (8)$$

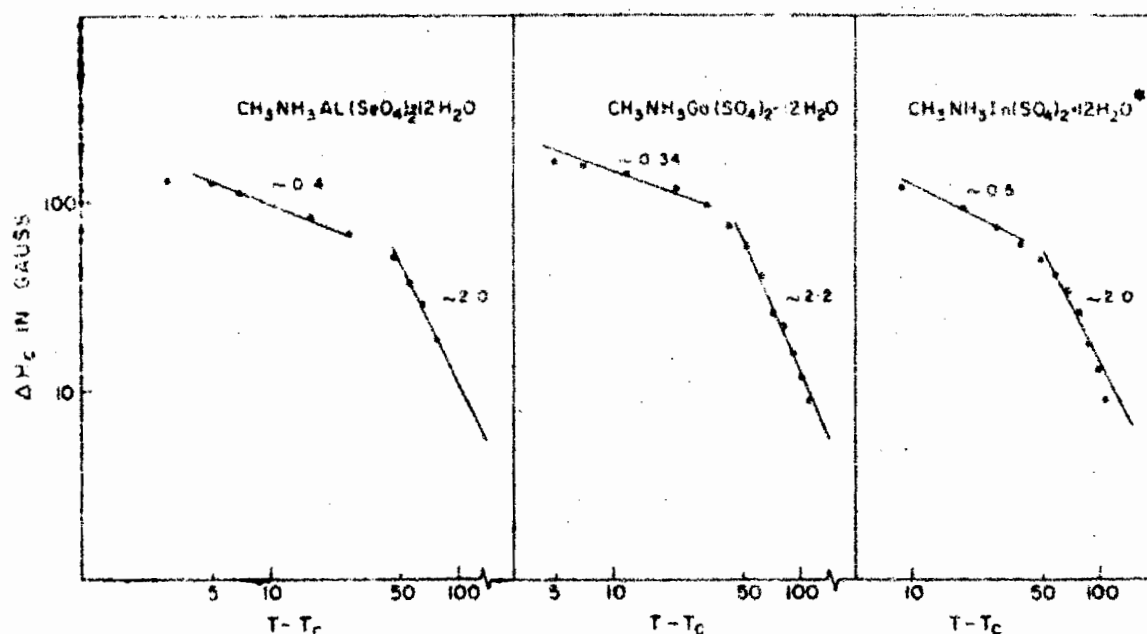


FIGURE 5 Shows the plot of ΔH_c against $(T - T_c)$ on a log-log scale for the three alums.

Near the phase transition temperature T_c one observes experimentally that (Figure 3.1) the satellite transitions are much broader than the central transition. This indicates that

$$12J^{(1)}(\omega) \ll 2J^{(0)} \quad (9)$$

From equation (9), it follows that

$$\tau_c > \omega^{-1}$$

where $\omega = 2\pi\gamma = 5.7 \times 10^{10} \text{ sec}^{-1}$, γ is the microwave frequency. At temperatures well above T_c , the observed line is Lorentzian and the correlation time τ_c associated with the fluctuation must be much shorter than $(\nu\delta D)^{-1}$. $\nu \sim 1.76 \times 10^7 \text{ sec}^{-1} \text{ G}^{-1}$ and δD must be of the order of satellite linewidth $\sim 200G$.

$$(\nu\delta D)^{-1} \sim 3 \times 10^{-10} \text{ sec.}$$

So, we can put an upper and a lower limit on the value of τ_c associated with fluctuation responsible for linewidth anomaly near the phase transition.

$$1.8 \times 10^{-11} \text{ sec} < \tau_c < 3 \times 10^{-10} \text{ sec} \quad (10)$$

Muller *et al.*⁷ have obtained static critical exponents in SrTiO_3 for the linewidth behaviour very close to T_c ($T_c = 105.6 \text{ K}$). Windsch *et al.*¹⁰ have also obtained results near T_c by making precise measurements of T_2 by electron spin echo method in Mn^{2+} : TSCC. However, in our case the experimental

* See reference (20).

limitations do not permit us to make such precise measurements very near T_c . Nevertheless, if one plots $\ln \Delta H_c$ vs. $\ln(T - T_c)$ (see Figure 5) one obtains some interesting results. ΔH_c is obtained by subtracting the background linewidth from the total linewidth. The plot shows that $\Delta H_c \sim (T - T_c)^{-n}$, where $n \sim 2$ for $T - T_c > 40 \text{ K}$ and $n \sim 0.4$ for $4 < (T - T_c) < 30 \text{ K}$. Similar results have been obtained by Nishimura *et al.*¹⁹ in the case of their EPR investigations of Cr^{3+} in triglycine sulfate.

Thus, we have seen that the critical fluctuations in the fine structure tensor lead to the linewidth anomaly of Cr^{3+} in the vicinity of T_c in the two ferroelectric alums considered. The major contribution to the fine structure term comes from the dipole moments of the six water molecules of the octahedron surrounding the trivalent ion.¹⁷ So, it seems water molecules play an important role in the mechanism of ferroelectricity in alums.

VI CONCLUSION

Electron paramagnetic resonance studies of Cr^{3+} in two ferroelectric alums show that there are four chemically equivalent and physically related sites per unit cell with axially symmetric D tensor at room temperature. EPR linewidth shows anomaly in the vicinity of T_c due to critical fluctuations. As a result of ferroelectric phase transition, EPR spectrum shows

a three-fold increase indicating the presence of three kinds of domains in the ferroelectric phase.

ACKNOWLEDGEMENTS

The authors express their appreciation of many helpful discussions with Professor B. Venkataraman and Professor R. Vijayaraghavan.

REFERENCES

1. A. Rigamonti, *Phys. Rev. Lett.* **19**, 436 (1967).
2. G. Bonera, F. Borsa and A. Rigamonti, *Phys. Rev.* **B2**, 2784 (1970).
3. R. Blinc and S. Zumer, *Phys. Rev. Lett.* **21**, 1004 (1968).
4. H. Unoki and T. Sakudo, *J. Phys. Soc. Japan*, **23**, 546 (1967).
5. K. A. Muller, W. Berlinger and F. Waldner, *Phys. Rev. Lett.* **21**, 814 (1968).
6. Th. von Waldkirch, K. A. Muller, W. Berlinger and H. Thomas, *Phys. Rev. Lett.* **28**, 503 (1972).
7. Th. von Waldkirch, K. A. Muller and W. Berlinger, *Phys. Rev.* **B7**, 1052 (1973).
8. V. V. Shapkin, B. A. Gromov, G. T. Petrov, Ya. G. Girschberg and E. V. Bursyan, *Fiz. tverd. Tela*, **15**, 1403 (1973).
9. G. Volkel, U. Bartuch, W. Brunner and W. Windsch, *Phys. Stat. Solidi (a)* **25**, 591 (1974).
10. G. Volkel, W. Brunner and W. Windsch, *Solid Stat. Comm.* **17**, 345 (1975).
11. D. E. O'Reilly and G. E. Schacher, *J. Chem. Phys.* **43**, 4222 (1965).
12. R. Pepinsky, F. Jona and G. Shirane, *Phys. Rev.* **102**, 1181 (1956).
13. A. Abragam and B. Bleaney, *Electron Paramagnetic Resonance of Transition Ions* (Clarendon Press, Oxford, 1970).
14. A. G. Danilov and A. Manoogian, *Phys. Rev.* **B6**, 4097 (1972).
15. D. M. S. Bagguley and J. H. E. Griffiths, *Proc. Roy. Soc. (London)* **A204**, 188 (1950).
16. F. Jona and G. Shirane, *Ferroelectric Crystals* (Pergamon Press, Inc., New York, 1962), Chapt. VIII.
17. D. E. O'Reilly and Tung Tsang, *Phys. Rev.* **157**, 417 (1967).
18. K. Nishimura and T. Hashimoto, *J. Phys. Soc. Japan*, **35**, 1699 (1973).
19. A. Abragam, *The Principles of Nuclear Magnetism* (Oxford University Press, London, 1961), pp. 313-315.
20. R. R. Navalgund and L. C. Gupta, *Phys. Stat. Solidi (b)* **71**, K87 (1975).